Decomposition and Construction of Cubic and Non-cubic Neighbourhood Operations

Atsushi Imiya[1,2]

[1]Super Computing Division, Institute of Management and Information Technologies, Chiba University

[2]Graduate School of Science and Engineering, Chiba University

Graphical Abstract

The properties of

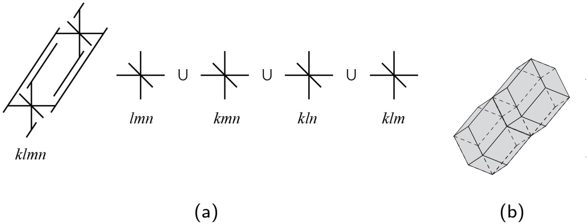

Figure 1: Decomposition of non-cubic grid.

are dealt with in this talk.

Summary

- Construct morphological operations in a higher-dimensional digital space from a collection of set operations in lower dimensional digital spaces is introduced.
- Morphological operations in an n-dimensional digital space can be computed as the union of one- and two-dimensional morphological operations.
- A class of non-cubic grid sysrems are projection of cubic grid system in a higher-dimensional space.
- The neighbourhood of the FCC-grid system is decomposed into four planar hexagonal neighbourfood.

Part of items 1 and 2 were first presented at the workshop on Discrete Topology and Mathematical Morphology in honor of the retirement of Gilles Bertrand on March 2019.
Item 4 is a solution to the question from J. Serra during the workshop.
Algebraic properties of rhombic dodecahaedron was derived by Troung Kieu Linh in her master thesis on 2004.

Contents

CHIBA UNIVERSITY

Example of Neighbourhood Decomposition

(a) Four-connected object on the digital plane.
(b) Neighbourhood operations on the horizontal isothetic lines on the digital plane.
(c) Neighbourhood operations on the vertical isothetic lines on the digital plane.

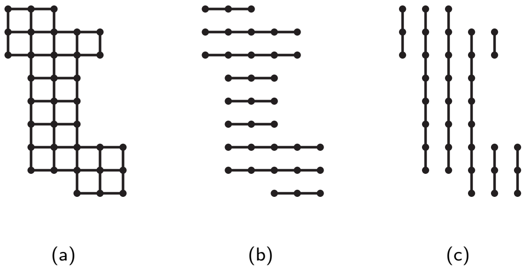

Figure 2: One-dimensional operations for a two-dimensional object.

2D and 3D Orthogonal Decompositions

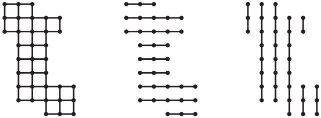

(a) (b) (c)

Figure 3: One-dimensional decomposition of the two-dimensional neighbourhood.

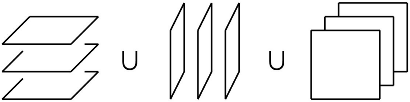

Figure 4: The multidirectional multislice decomposition of a digital point set in a three-dimensional digital space.

3D and 4D Orthogonal Decomposition

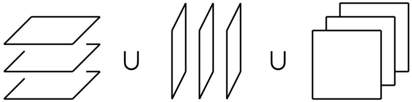

Figure 5: The multidirectional multislice decomposition of a digital point set in a three-dimensional digital space.

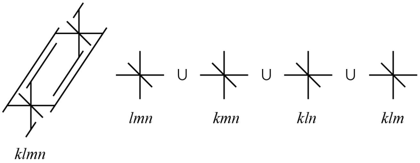

Figure 6: The 8-neighbourhood in a four-dimensional digital space is decomposed into four mutually orthogonal 6-neighbourhoods in the three-dimensional digital spaces.

Hierarchical Relations of Decomposition

$$
\begin{aligned}
\mathbf{N}^n &= \bigcup_{k=1}^{n} \mathbf{N}_k^{n-1}, \\
& \quad \mathbf{N}_k^{n-1} = \mathbf{N}^n \setminus \mathbf{N}_k^1, \\
\mathbf{N}_k^{n-1} &= \bigcup_{l=1}^{n-1} \mathbf{N}_{kl}^{n-2}, \\
& \quad \mathbf{N}_{kl}^{n-2} = \mathbf{N}_k^{n-1} \setminus \mathbf{N}_l^1, \\
\mathbf{N}_{kl}^{n-2} &= \bigcup_{m=1}^{n-2} \mathbf{N}_{klm}^{n-3}, \\
& \quad \mathbf{N}_{klm}^{n-3} = \mathbf{N}_{kl}^{n-2} \setminus \mathbf{N}_m^1.
\end{aligned}
$$

Recursive Form

From the linear neighbourhood in $\mathbf{Z}^n$ such that

$$\mathbf{N}_k^1 = \{\boldsymbol{x} \,|\, |x_k| = 1,\ x_i = 0,\ i \neq k\}, \tag{1}$$

we can construct $\mathbf{N}^n$ as

$$\mathbf{N}^n = \bigcup_{k=1}^{n} \mathbf{N}_k^1 \tag{2}$$

For $l = 0, 1, \cdots, n-1$,

$$\begin{aligned} \mathbf{N}^{n-l}_{k(1)k(2)\cdots k(l)} &= \bigcup_{k(l)=1}^{n-l} \mathbf{N}^{n-(l+1)}_{k(1)k(2)\cdots k(l+1)}, \\ \mathbf{N}^{n-(l+1)}_{k(1)k(2)\cdots k(l+1)} &= \mathbf{N}^{n-l}_{k(1)k(2)\cdots k(l)} \setminus \mathbf{N}^1_{k(l+1)}. \end{aligned} \tag{3}$$

Set Decomposition

For $l = 0, 1, 2, \cdots, n-1$

$$\mathbf{F}_{k(l)\alpha(l)} = \bigcup_{k(l)=1}^{n-l} \left(\bigcup_{\alpha(l)\in\mathcal{N}(k(l))} \mathbf{F}_{k(l)\alpha(l)} \right) \tag{4}$$

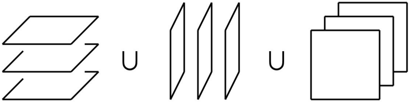

Figure 7: The multidirectional multislice decomposition of a digital point set in a three-dimensional digital space.

Digital Objects

Setting $\mathbf{R}^n$ to be an n-dimensional Euclidean space,

$$\boldsymbol{x} = (x_1, x_2, \cdots, x_n)^\top \in \mathbf{R}^n$$

Definition

Let $\mathbf{Z}$ be the set of all integers. The n-dimensional digital space $\mathbf{Z}^n$ is set of all $\boldsymbol{x}$ for which all x_i are integers.

Definition

The voxels centred at the point $\boldsymbol{y} \in \mathbf{Z}^n$ in $\mathbf{R}^n$ is

$$\mathbf{V}(\boldsymbol{y}) = \left\{ \boldsymbol{x} \,\middle|\, |\boldsymbol{x} - \boldsymbol{y}|_\infty \leq \frac{1}{2} \right\}. \tag{5}$$

Point Sets and Voxels

(a) Voxel in $\mathbf{R}^3$.
(b) The 6-neighbourhood in $\mathbf{Z}^3$.
(c) The 6-connected voxels in $\mathbf{R}^3$.

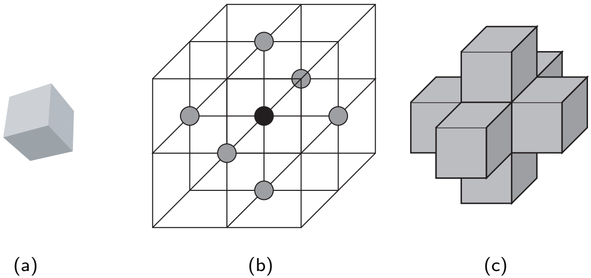

Figure 8: Two expressions of digital images

Digital Simplex and Complex

Let $\boldsymbol{e}_k$ be the unit vector whose kth element is 1. The digital n-simplex with $2n$-connectivity in $\mathbf{Z}^n$ is

$$\mathbf{S} = \left\{ \boldsymbol{v}(\varepsilon_1, \varepsilon_2, \cdots, \varepsilon_n) \,\middle|\, \boldsymbol{v}(\varepsilon_1, \varepsilon_2, \cdots, \varepsilon_n) = \sum_{k=1}^{n} \varepsilon_k \boldsymbol{e}_i, \ \ \varepsilon_i \in \{0, 1\} \right\}. \quad (6)$$

We define the digital n-complex using $\mathbf{S}$.

Definition

The digital n-complex is a union of connected simplices.

Definition

The digital thick n-complex is a union of simplices connected by $(n-1)$-simplices.

Using digital thick n-complices, we define a digital object.

Definition

If the number of connected simplices in a thick n-complex $\mathbf{F}$ is finite and if the complement of $\mathbf{F}$ is a thick n-complex, we call $\mathbf{F}$ a digital object.

Operations to 1D Object

Example

On $\mathbf{Z}$, a digital object is a finite union of finite intervals

$$\mathbf{I} = \bigcup_{i=1}^{n} \mathbf{I}_i, \quad \mathbf{I}_i = [a_i, b_i] \tag{7}$$

for $a_i < a_{i+1}$ and $b_i < b_{i+1}$ with the condition $(a_{i+1} - b_i) \geq 3$.

Example

The dilation and erosion of a collection of points are concatenation and elimination of points to both endpoints of a string, respectively, such that

$$\mathbf{O} \oplus \mathbf{N}^1 = \{k\}_{n-1}^{m+1}, \quad \mathbf{O} \ominus \mathbf{N}^1 = \{k\}_{n+1}^{m-1}, \tag{8}$$

assuming $(m-1) + (n+1) \geq 0$.

CHIBA UNIVERSITY

1D Object

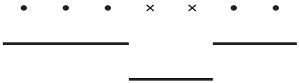

Figure 9: Operation on a digital line.

$$\mathbf{I} = \bigcup_{i=1}^{n} \mathbf{I}_i, \quad \mathbf{I}_i = [a_i, b_i]$$

for $a_i < a_{i+1}$ and $b_i < b_{i+1}$ with the condition $(a_{i+1} - b_i) \geq 3$.

Thickness and Thinness of Objects

Definition

We call a connected component of k-simplices for $k \leq (n-1)$ a thin object.

The minimum thickness of a thin object is one.

Definition

The digital n-complex is a union of connected simplices.

Definition

The digital thick n-complex is a union of simplices connected by $(n-1)$-simplices.

Definition

If the number of connected simplices in a thick n-complex $\mathbf{F}$ is finite and if the complement of $\mathbf{F}$ is a thick n-complex, we call $\mathbf{F}$ a digital object.

Digital Objects and Nef Polytope

Definition

For an object $\mathbf{F} \in \mathbf{Z}^n$, the embedding of $\mathbf{F}$ into $\mathbf{R}^n$ is

$$\mathcal{F} = \bigcup_{\boldsymbol{x} \in \mathbf{F}} \mathbf{V}(\boldsymbol{x}). \tag{9}$$

Definition

The dual grid

$$\mathbf{D}^n = \mathbf{Z}^n + \left\{ \frac{1}{2}\boldsymbol{e} \right\}, \quad \boldsymbol{e} = \sum_{i=1}^{n} \boldsymbol{e}_i \tag{10}$$

of $\mathbf{Z}^n$.

Lemma

The polytope $\mathcal{F}$ is an isothetic Nef-polytope, which is a union of voxels connected by the faces of voxels. The vertices of $\mathcal{F}$ lie on the dual grid.

2D Operation

(a) Union of the internal and external boundaries.
(b) Refinement operations at the corners preserve the continuity of the internal and external boundaries.

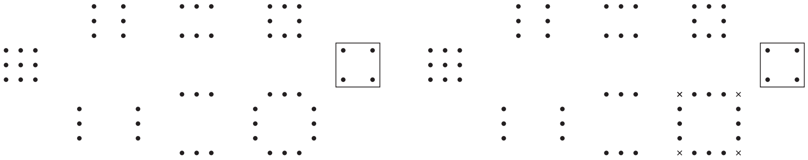

(a) (b)

Figure 10: Refinement operation and boundary detection.

Boundary of Digital and Discrete Objects

Definition

The internal and external boundaries of the point set $\mathbf{F}$ are

$$\begin{aligned} \partial_{-}\mathbf{F} &= \mathbf{F} \setminus (\mathbf{F} \ominus \mathbf{N}^n) && (11) \\ \partial_{+}\mathbf{F} &= (\mathbf{F} \oplus \mathbf{N}^n) \setminus \mathbf{F} && (12) \end{aligned}$$

Definition

The digital set gradient on the boundary is

$$\partial\mathbf{F} = \left(\bigcup_{\boldsymbol{x} \in \overline{\partial_{+}\mathbf{F}}} \mathbf{V}(\boldsymbol{x}) \right) \bigcap \left(\bigcup_{\boldsymbol{x} \in \overline{\partial_{-}\mathbf{F}}} \mathbf{V}(\boldsymbol{x}) \right). \qquad (13)$$

CHIBA UNIVERSITY

Refinement Operation

The singular points disturb the connectivity along the boundary curves.
The refined internal and external boundaries prevent the continuity.

Definition

The singular points are

$$\mathbf{C}_- = (\partial_-\overline{\mathbf{F}} \bigcup \partial_+\mathbf{F}) \setminus (\partial_-\overline{\mathbf{F}} \bigcap \partial_+\mathbf{F}), \tag{14}$$

$$\mathbf{C}_+ = (\partial_+\overline{\mathbf{F}} \bigcup \partial_-\mathbf{F}) \setminus (\partial_+\overline{\mathbf{F}} \bigcap \partial_-\mathbf{F}). \tag{15}$$

Definition

The refinements are

$$\overline{\partial_-\mathbf{F}} = \partial_-\mathbf{F} \bigcup \mathbf{C}_-, \tag{16}$$

$$\overline{\partial_+\mathbf{F}} = \partial_+\mathbf{F} \bigcup \mathbf{C}_+. \tag{17}$$

Minkowski Operations and Set Operations

For the Minkowski addition and subtraction, the relations

$$\mathbf{F} \ominus \mathbf{G} = \overline{\mathbf{F} \oplus \overline{\mathbf{G}}}, \tag{18}$$

$$\mathbf{F} \oplus (\mathbf{G} \cup \mathbf{H}) = (\mathbf{F} \oplus \mathbf{G}) \cup (\mathbf{F} \oplus \mathbf{H}), \tag{19}$$

$$\mathbf{F} \ominus (\mathbf{G} \cup \mathbf{H}) = (\mathbf{F} \ominus \mathbf{G}) \cap (\mathbf{F} \ominus \mathbf{H}) \tag{20}$$

are satisfied. Furthermore, we obtain the following lemma.

Lemma

If $\mathbf{F} \cap \mathbf{G} = \emptyset$, the equalities

$$(\mathbf{F} \cup \mathbf{G}) \oplus \mathbf{H} = (\mathbf{F} \oplus \mathbf{H}) \cup (\mathbf{G} \oplus \mathbf{H}), \tag{21}$$

$$(\mathbf{F} \cup \mathbf{G}) \ominus \mathbf{H} = (\mathbf{F} \ominus \mathbf{H}) \cup (\mathbf{G} \ominus \mathbf{H}) \tag{22}$$

are satisfied.

Recursive Forms

Theorem

The boundary $\partial_{\pm}\mathbf{F}$ of an n-dimensional digital object $\mathbf{F}$ is the union of its $(n-1)$-dimensional boundaries.

For $l = 0, 1, \cdots, n-1$,

$$\mathbf{F}_{k(l)\alpha(l)} \setminus (\mathbf{F}_{k(l)\alpha(l)} \ominus \mathbf{N}^{n-l}_{k(1)k(2)\cdots k(l)}) = \bigcup_{k(l+1)=1}^{n-l} \bigcup_{\alpha(l+1)\in\mathcal{N}(k(l+1))} \left(\mathbf{F}_{k(l+1)\alpha(l+1)} \setminus (\mathbf{F}_{k(l+1)\alpha(l+1)} \ominus \mathbf{N}^{n-l}_{k(1)k(2)\cdots k(l+1)})\right), \tag{23}$$

$$(\mathbf{F}_{k(l)\alpha(l)} \oplus \mathbf{N}^{n-l}_{k(1)k(2)\cdots k(l)}) \setminus \mathbf{F}_{k(l)\alpha(l)} = \bigcup_{k(l+1)=1}^{n-l} \bigcup_{\alpha(l+1)\in\mathcal{N}(k(l+1))} \left((\mathbf{F}_{k(l+1)\alpha(l+1)} \oplus \mathbf{N}^{n-l}_{k(1)k(2)\cdots k(l+1)}) \setminus \mathbf{F}_{k(l+1)\alpha(l+1)}\right) \tag{24}$$

1D Operation for Boundary Detection

$\partial_{\pm}\overline{\mathbf{F}}$ is numerically computed by

$$\partial_{\pm}\overline{\mathbf{F}} = \{\partial_{\pm}(\mathbf{H} \setminus \mathbf{F})\} \setminus \partial_{\pm}\mathbf{F} \quad (25)$$

for a large hypercube $\mathbf{H}$, which encloses $\mathbf{F}$ with the condition

$$\min_{\boldsymbol{x}\in(\mathbf{H}\setminus\mathbf{F}),\boldsymbol{y}\in\mathbf{F}} |\boldsymbol{x}-\boldsymbol{y}| \geq 3 \quad (26)$$

on the isothetic lines $\boldsymbol{z} = \boldsymbol{a} + t\boldsymbol{e}_i$ for $\boldsymbol{a} \in \mathbf{Z}^n$.

Perfect Objects and Well-composed Sets

Definition

For a thin object $\mathbf{T}$ in $\mathbf{Z}^n$, we call the embedding of $\mathbf{T}$ in $\mathbf{R}^n$

$$\mathcal{T} = \bigcup_{\boldsymbol{x} \in \mathbf{T}} \mathbf{V}(\boldsymbol{x}) \tag{27}$$

an imperfect voxel object.

Definition

In $\mathbf{R}^n$, if the complement of voxel object $\mathcal{P}$ is an imperfect voxel object, we call $\mathcal{P}$ a perfect voxel object.

Theorem

In a perfect voxel object any imperfect voxel object is contained as connected components, although imperfect voxel objects are permissible for embedding of point sets based on the well-composed sets.

Perfect Objects and Well-composed Sets

Theorem

The closure of $[\partial \mathbf{F}] = [\partial \mathcal{F}]$ *is an* n*-complex in the dual grid.*

Theorem

The thickness of the complement of $[\partial \mathbf{F}] = [\partial \mathcal{F}]$ *is at least two voxels.*

Theorem

An isothetic Nef-polytope $\mathcal{F}$ *and its complement are perfect voxel objects.*

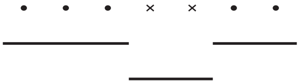

Figure 11: Perfect object on a digital line.

Resampling

Since a sub-grid point $\boldsymbol{p}$ in the unit hypercube $[0,1]^n$ is expressed as

$$\boldsymbol{p} = \sum_{i=1}^{n} \frac{\alpha(i)}{k} \boldsymbol{e}_i, \tag{28}$$

for $\alpha(i) = 0, 1, 2, \cdots, n-1$, where k is an appropriate positive integer, we have the following definition.

Definition

The k-sub-grid is

$$\mathbf{Z}_k^n = \left\{ \boldsymbol{y} | \boldsymbol{y} = \boldsymbol{x} + \sum_{i=1}^{n} \frac{\alpha(i)}{k} \boldsymbol{e}_i,\ \boldsymbol{x} \in \mathbf{Z}^n \right\} \tag{29}$$

Definition

The resampling of $\mathcal{F} \in \mathbf{R}^n$ in the k-sub-grid $\mathbf{Z}_k^n$ is expressed as $\mathbf{F}^k$.

Theorem

If an object is connected in k-sub-grid, the object is k well-composed. Three well-composedness is well-composedness

Digital Curvature Codes

For $ci_i \in \{+1, -1, 0, \emptyset\}$, in $\mathbf{Z}^n$ $n \geq 3$,

$$\gamma_n(\boldsymbol{x}) = \langle \gamma_1, \gamma_2 \cdot \cdots \gamma_n \rangle. \quad (30)$$

- 3 configurations $\gamma_2(\boldsymbol{x}) \in \{+1, 0, -1\}$ in $\mathbf{Z}^2$.
- 9 configurations in $\mathbf{Z}^3$.
- $f(n)$ configurations in $\{\mathbf{Z}\}^{\mathbf{n}}$, where $f(n)$ is the number of bi-partitions of the 3^n-digital cube, using the $2n$-connectivity in $\mathbf{Z}^n$.

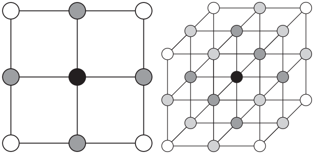

(a) (b)

Figure 12: 3^n point sets in $\mathbf{Z}^2$ and $\mathbf{Z}^3$.

Rhombic Dodecahedron as Voronoi Tessellation in FCC-Grid System

Rhombic dodecahedra are the voxels for the face centred grid system.
Hexagons are pixels for the hexagonal grid system.
They are derived as Voronoi tessellation of grid systems.

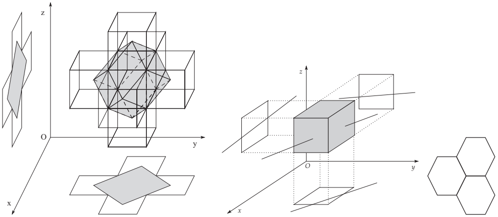

(a) (b) (c)

Figure 13: Cube, rhombic dodecahedron and hexagons. (a) and (b) are voxels and their projections to planes perpendicular to vectors $\boldsymbol{e}_3 = (0,0,1)^\top$ and $\boldsymbol{e}_2 = (0,1,0)^\top$.

Vertices of Rhombic Dodecahedron

In Figure 13, fourteen vertices of the rhombic dodecahedron $R_{kmn}((x_k, y_m, z_n)^\top)$ centred at the point $(x_k, y_m, z_n)^\top \in \mathbf{Z}^3$ are

$$
\begin{array}{ll}
(x_k, y_m, z_n - 1)^\top, & (x_k, y, z_n + 1)^\top, \\
(x_k, y_m - 1, z_n)^\top, & (x_k, y_m + 1, z_n)^\top, \\
(x_k - 1, y_m, z_n)^\top, & (x_k + 1, y_m, z_n)^\top, \\
(x_k + \frac{1}{2}, y_m - \frac{1}{2}, z_n - \frac{1}{2})^\top, & (x_k + \frac{1}{2}, y_m - \frac{1}{2}, z_n + \frac{1}{2})^\top, \\
(x_k + \frac{1}{2}, y_m + \frac{1}{2}, z_n \frac{1}{2})^\top, & (x_k + \frac{1}{2}, y_m + \frac{1}{2}, z_n + \frac{1}{2})^\top, \\
(x_k - \frac{1}{2}, y_m - \frac{1}{2}, z_n - \frac{1}{2})^\top, & (x_k - \frac{1}{2}, y_m - \frac{1}{2}, z_n + \frac{1}{2})^\top, \\
(x_k - \frac{1}{2}, y_m + \frac{1}{2}, z_n - \frac{1}{2})^\top, & (x_k - \frac{1}{2}, y_m + \frac{1}{2}, z_n + \frac{1}{2})^\top.
\end{array}
\tag{31}
$$

Eight vertices out of fourteen have three adjacent edges. These eight vertices form a cube. Therefore, tetrahedrons are contained in this cube.

CHIBA UNIVERSITY

Voronoi Tessellation in FCC-Grid System

The rhombic-dodecahedral voxel is interior defined by the system of double inequalities

$$\begin{cases} x_k + y_m - 1 \leq x + y \leq x_k + y_m + 1 \\ x_k - y_m - 1 \leq x - y \leq x_k - y_m + 1 \\ y_m + z_n - 1 \leq y + z \leq y_m + z_n + 1 \\ y_m - z_n - 1 \leq y - z \leq y_m - z_n + 1 \\ x_k + z_n - 1 \leq x + z \leq x_k + z_n + 1 \\ x_k - z_n - 1 \leq x - z \leq x_k - z_n + 1. \end{cases} \tag{32}$$

This expression is derived by Troung Kieu Linh.

Connectivity of Rhombic-dodecahedral Voxels 1

A 3D space is filled by rhombic dodecahedra whose centres lie on planes

$$\{(x_k, y_m, z_n)^\top | x_k + y_m + z_n = 2k\} \vee \{(x_k, y_m, z_n)^\top | x_k + y_m + z_n = 2k+1\} \quad (33)$$

Property

A pair of rhombic dodecahedra $R_{kmn}((x_k, y_m, z_n)^\top)$ and $R_{\alpha\beta\gamma}((x_\alpha, y_\beta, z_\gamma)^\top)$, whose centres are $(x_k, y_m, z_n)^\top$ and $(x_\alpha, y_\beta, z_\gamma)^\top$, respectively, are face-connected if they share a face for a pair of planes

$$\begin{cases} x_k + y_m + z_n = 2k_0 \\ x_\alpha + y_\beta + z_\gamma = 2l_0 \end{cases} \vee \begin{cases} x_k + y_m + z_n = 2k_0 + 1 \\ x_\alpha + y_\beta + z_\gamma = 2l_0 + 1 \end{cases} \quad (34)$$

as shown in Figure 14 (a) for integers k_0 and l_0

Connectivity of Rhombic-dodecahedral Voxels 2

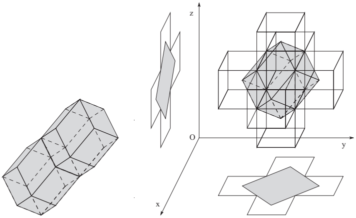

(a) (b)

Figure 14: Face connection of rhombic dodecahedral-voxels

Algebraic an Geometrical Properties of Space-filling

Property

Same properties for face connectivity of a pair of rhombic dodecahedra are satisfied for

$$\begin{cases} x_k + y_m - z_n = 2k_1 \\ x_\alpha + y_\beta - z_\gamma = 2l_1 \end{cases} \vee \begin{cases} x_k + y_m - z_n = 2k_1 + 1 \\ x_\alpha + y_\beta - z_\gamma = 2l_1 + 1 \end{cases}$$

$$\begin{cases} x_k - y_m + z_n = 2k_2 \\ x_\alpha - y_\beta + z_\gamma = 2l_2 \end{cases} \vee \begin{cases} x_k - y_m + z_n = 2k_2 + 1 \\ x_\alpha - y_\beta + z_\gamma = 2l_2 + 1 \end{cases} \quad (35)$$

$$\begin{cases} x_k - y_m - z_n = 2k_3 \\ x_\alpha - y_\beta - z_\gamma = 2l_3 \end{cases} \vee \begin{cases} x_k - y_m - z_n = 2k_3 + 1 \\ x_\alpha - y_\beta - z_\gamma = 2l_3 + 1 \end{cases}$$

where k_i and l_i are integers for $i = 1, 2, 3$.

Slices of Rhombic Dodecahedron

Intersection of $R_{kmn}((x_k, y_m, z_n)^\top)$ and

$$\begin{cases} x_k + y_m + z_n = 2k_0 = \boldsymbol{p}_0^\top \boldsymbol{x} \\ x_k + y_m - z_n = 2k_1 = \boldsymbol{p}_{-1}^\top \boldsymbol{x} \\ x_k - y_m + z_n = 2k_2 = \boldsymbol{p}_{-2}^\top \boldsymbol{x} \\ x_k - y_m - z_n = 2k_3 = \boldsymbol{p}_3^\top \boldsymbol{x}, \end{cases} \quad (36)$$

for

$$\begin{aligned} \boldsymbol{p}_0 &= (1,1,1)^\top, \\ \boldsymbol{p}_1 &= (-1,-1,1)^\top, \\ \boldsymbol{p}_2 &= (-1,1,-1)^\top, \\ \boldsymbol{p}_3 &= (1,-1,-1)^\top \end{aligned} \quad (37)$$

are regular hexagons, where and $\boldsymbol{p}_{-i} = -\boldsymbol{p}_i$.

Vertex-first Projection of Rhombic Dodechedron

Three dimensional linear subspaces

$$\mathbf{R}^3_{\perp \boldsymbol{p}_i^4} = \{\boldsymbol{x} \,|\, \boldsymbol{p}_i^{4\top}\boldsymbol{x} = 0, \boldsymbol{x} \in \mathbf{R}^4\} \tag{38}$$

which are perpendicular to the vectors

$$\begin{array}{ll} \boldsymbol{p}_0^4 = (1,1,1,1)^\top, & \boldsymbol{p}_1^4 = (1,-1,1,1)^\top, \\ \boldsymbol{p}_2^4 = (1,1,-1,1)^\top, & \boldsymbol{p}_3^4 = (1,1,1,-1)^\top, \\ \boldsymbol{p}_4^4 = (1,1,-1,-1)^\top, & \boldsymbol{p}_5^4 = (1,-1,1,-1)^\top, \\ \boldsymbol{p}_6^4 = (1,1,-1,-1)^\top, & \boldsymbol{p}_7^4 = (1,-1,-1,-1)^\top \end{array}$$

are the rhombic-dodecahedral space filling.

$$\mathbf{R}^3_{\perp \boldsymbol{p}_i^3} = \{\boldsymbol{x} \,|\, \boldsymbol{p}_i^{3\top}\boldsymbol{x} = 0, \boldsymbol{x} \in \mathbf{R}^4\} \tag{39}$$

which are perpendicular to the vectors

$$\begin{array}{ll} \boldsymbol{p}_0^3 = (1,1,1)^\top, & \boldsymbol{p}_1^3 = (1,1,-1)^\top, \\ \boldsymbol{p}_2^3 = (1,-1,1)^\top, & \boldsymbol{p}_3^3 = (1,-1,-1)^\top. \end{array}$$

are hexagonal tilling.

Decomposition of Neighbourhood in FCC Grid to These in Hexagonal Grids

Theorem

Setting $\mathbf{H}^6_{\boldsymbol{p}_i^\perp}$ *to be the hexagonal grid system on the plane perpendicular to the vector* $\boldsymbol{p}_i$, *for*

$$\begin{array}{ll} \boldsymbol{p}_0 = (1,1,1,)^\top, & \boldsymbol{p}_1 = (-1,-1,1,)^\top, \\ \boldsymbol{p}_2 = (-1,1,-1,)^\top, & \boldsymbol{p}_3 = (1,-1,-1,)^\top \end{array}$$

the decomposition of FCC grit to planar hexagonal grid is

$$\mathbf{F}^{14}(\boldsymbol{x}) = \bigcup_{i=0}^{3} \mathbf{H}^6_{\boldsymbol{p}_i^\perp}(\boldsymbol{x}) \tag{40}$$

Decomposition of Hexagonal Connectivity

Setting

$$\boldsymbol{v}_k = \left(\cos\left(\frac{\pi}{3}k + \frac{\pi}{4}\right), \sin\left(\frac{\pi}{3}k + \frac{\pi}{4}\right)\right)^\top \tag{41}$$

to be six vertices of a hexagon centred at the origin, The hexagonal neighbourhood is decomposed as

$$\mathbf{H}_2^6(0) = \bigcup_{k=0}^{2} \mathbf{N}_1^2[2k] \tag{42}$$

for

$$\mathbf{N}_1^2[2k] = \{-2\boldsymbol{w}_k, 0, 2\boldsymbol{w}_k\} \tag{43}$$

where

$$\boldsymbol{w}_k = \frac{1}{2}(\boldsymbol{v}_{2k} + \boldsymbol{v}_{2k+1})$$

Results, Comments and Perspectives

- Decomposition of the $2n$-neighbourhood in an n-dimensional digital space into the $2(n-1)$-neighbourhoods in the mutually orthogonal $(n-1)$-dimensional digital spaces
- Construction of the object boundary in an n-dimensional digital space form the digital boundaries in the mutually orthogonal $(n-1)$-dimensional digital spaces
- In 2- and 3-dimensional spaces, decomposition and construction derive the digital curvature on digital manifolds
- How can we define the curvature codes in n-dimensional digital space?
- Decomposition by projections in higher-dimensional non-cubic grid system.
    - Vertex-first projection of 4-cube is the rhombic dodecahedron.
    - Projection of 3-cube is the hexagon.
    - Projection of rhombic dodecahedron is hexagon.

CHIBA UNIVERSITY

References

1. Innchyn Her: Geometric transformations on the hexagonal grid, IEEE Trans. Image Processing, **4**, 1213-1222, (1995)
2. Innchyn Her: Description of the F.C.C.lattice geometry through a four-dimensional hypercube, Acta Crystallographica Section A, **51**, 659-662, (1995)
3. Lidija Čomić, Benedek Nagy: A topological 4-coordinate system for the face centered cubic grid, Pattern RecoPattern Recognnition Letters, **83**, 67-74, (2016)
4. Lidija Čomić, Paola Magillo: Repairing 3D binary images using the FCC grid, Journal of Mathematical Imaging and Vision, **61**, 1301-1321, (2019)
5. Nicolas Boutry, Thierry Géraud, Laurent Najman: A Tutorial on well-composedness, Journal of Mathematical Imaging and Vision, **60**, 443-478, (2018)
6. Atsushi Imiya: Decomposition and construction of higher-dimensional neighbourhood operations, Pattern Recognnition Letters, **135**, 321-328, (2020)
7. Robin Strand, Gunilla Borgefors: Resolution pyramids on the FCC and BCC grids, in Eric Andres Guillaume Damiand, Pascal Lienhardt P. (eds) Discrete Geometry for Computer Imagery:DGCI2005, Lecture Notes in Computer Science, **3429**, Springer, Berlin, Heidelberg, (2005)

CHIBA UNIVERSITY